Int. J. Therm. Sci. (2001) 40, 1–10

S1290-0729(00)01180-7/FLA

Dynamics of a bifurcating flow within an open heated cavity

Lionel Lalanne, Yves Le Guer, René Creff *

Laboratoire de Transferts Thermiques, Équipe d'accueil 1932, Hélioparc, Avenue Angot, 64000 Pau, France

(Received 22 September 1999, accepted 3 February 2000)

Abstract — A numerical study of a 2D jet, confined in a heated or nonheated "horse shoe" cavity containing a bluff body is presented. Over critical conditions, this system exhibits self-sustained oscillations with well defined saturated amplitude and frequencies. Through the oscillating velocity amplitudes and the phenomenon frequencies, we defined a global mode. A universal curve for both streamwise and spanwise renormalized amplitudes emphasizes this global behavior. The stabilizing effect of the heated wall boundaries is shown. As an example, a delay of 6 % for $\Delta T = 10$ K, the temperature difference between the walls and the working fluid, raises the onset of the self-sustained mechanism. The global mode conservation with heating boundaries proves that the confined jet is insensitive to external perturbation such as heating. © 2001 Éditions scientifiques et médicales Elsevier SAS

instability / Hopf bifurcation / oscillation frequency / thermal stabilization / global mode

Nomenclature

a	thermal diffusivity	$m^2 \cdot s^{-1}$
A	velocity amplitude	$m \cdot s^{-1}$
d	nozzle width	m
$D*/dt$	total time derivative	
Δ	Laplacian operator	
f	fundamental frequency	Hz
h	nozzle depth	m
P	pressure	Pa
t	time	s
u	longitudinal velocity	$m \cdot s^{-1}$
U	inlet velocity	$m \cdot s^{-1}$
v	transverse velocity	$m \cdot s^{-1}$
x	longitudinal coordinate	m
y	transverse coordinate	m
T_{inlet}	inlet temperature	K
T_{wall}	wall temperature	K
α	slope	Hz
ν	kinematic viscosity	$m^2 \cdot s^{-1}$
μ	dynamic viscosity	Pa·s
Re	Reynolds number $= Ud/\nu$	
St	Strouhal number $= fd/U$	

* Correspondence and reprints.
E-mail addresses: lionel.lalanne@univ-pau.fr (L. Lalanne), rene.creff@univ-pau.fr (R. Creff).

1. INTRODUCTION

Since the nineteenth century, because of their considerable practical importance, the problems related to hydrodynamic stability were analyzed and formulated. Many authors clearly described mechanisms of instabilities.

The periodic unsteady flows can be separated in two types, called "open" and "closed" flows. A flow is "closed" when the fluid particles are recycled in the physical domain. A flow is "open", from a kinematic point of view, if all the present particles leave the domain. For example, Poiseuille flow, wakes are "open" systems whereas Rayleigh–Bénard flow confined within two horizontal plates is a "closed" system. In terms of hydrodynamic stability, "closed" and "open" flows are defined in terms of "absolutely unstable" and "convectively unstable", respectively. A flow is referred as absolutely unstable if after an initial impulse a disturbance grows in time at any spatial location. If this disturbance is ultimately convected away, one speaks about convective instability.

This concept of unstable wave propagation, first introduced in the study of plasma instabilities, is here applied to aerodynamic and hydrodynamic instabilities. For a given flow, the two different points of view can be inter-

dependent. Huerre [1] gives the example of a parallel axisymmetric hot jet which is absolutely unstable when the core temperature is sufficiently higher than the ambient temperature whereas a cold jet is considered convectively unstable. Although fluid particles move downstream, hydrodynamic instability, in the case of the hot jet, affects the entire domain of interest.

The aim of this paper is not to find a criterion which can help us to determine if a flow is convectively or absolutely unstable, but to characterize the evolution of a given flow in a physical domain with the changes of a control parameter such as the Reynolds number. *Re* represents a bifurcation parameter, which means that the flow reaches a new state of equilibrium above a particular Reynolds number value.

Many researchers studied the possible connections between local absolute instability and self-excited or noise amplified phenomenon, sustained by the experimental discovery made by Provansal et al. [2] applied itself to the description and the characterization of the flow dynamics. Since then, studies of this type have been repeated and refined, leading, for instance, to the transient experiments method (Monkewitz et al. [3]), a measure of the response of the wake to an impulsive change of the bifurcation parameter.

Through Sonhauss' works about edge-tones, researchers observed the self-excited mechanisms and their possible applications. Rockwell and Naudasher [4] present many configurations of impinging free shear layers inducing such a phenomenon. Our work presented here is in keeping with this general pattern and is developed in order to improve systems of flow measurement. Fluidic metering has been of particular interest because of its low-flow measurement ability. Over a critical Reynolds number, the confined jet oscillates on both sides of the symmetry axis. The frequency of this phenomenon is easily linked to the inlet velocity.

Further works focused on methods of suppressing, altering or delaying the onset of those structures from self-excited mechanisms. In the case of a hot round jet (Yu and Monkewitz [5]) the heating makes the jet sensitive to external forcing. Roussopoulos [6] found in his experiments that dynamic feedback control allows the delay of the wake instability onset about 20 % with respect to the Reynolds number than without control. Jointly to our dynamic study, we focused on the influence of the boundary temperature on the onset of the bifurcation. The general pattern of the flow is also investigated in this case.

The aim of this paper is various. First, in section 2, we briefly present the computational domain, we explain the boundaries and initial conditions. The history points where the time evolutions of the velocity fields are stored are also summarized. Second, in section 3, we extend the great deal of attention which had been paid to wake flows from confined jets. We show that under supercritical conditions, following the linear theory behavior, a disturbance increases exponentially in time and reaches a temporally periodic behavior, often called "limit cycle". Third, in section 4, we show the global nature of the entire flow field. Then, in section 5, we present additional works where the self-sustained phenomenon, through its global mode, can be influenced by heating the boundary domain.

2. NUMERICAL METHOD AND COMPUTATIONAL DOMAIN

The unsteady Navier–Stokes equations were solved with the Fluent code using the finite volume method in agreement with the following assumptions: the flow is an incompressible 2D jet, the working fluid (air at standard conditions) is Newtonian and homogeneous. The governing equations are:

$$\rho\frac{\mathrm{D}\boldsymbol{U}}{\mathrm{D}t} + \mathbf{grad}P = \mu(T)\Delta\boldsymbol{U}$$
$$\mathrm{div}\,\boldsymbol{U} = 0$$
$$\frac{\mathrm{D}T}{\mathrm{D}t} = a(T)\Delta T$$

The physical domain presented in *figure 1* is composed with a rectangular slit inlet called "nozzle", a "horse shoe" shape chamber including a bluff body crosswise to the main direction of the flow. This chamber is 100 mm long and 170 mm wide. The ratio aspect is defined as $a = d/h = 1/7$, with h the depth of the domain and d the nozzle width. We compute the governing equations following only two dimensions: $[Ox)$ streamwise and $[Oy)$ spanwise. This assumption is checked experimentally as long as $a > 1/5$. The bluff body is 30 mm long (in its largest dimension) and 110 mm wide. It has a 40 mm diameter hemispherical cavity. We have shown, in an additional work, that the presence of this central cavity is required for the appearance of the self-excited phenomenon.

The boundary conditions have been chosen in the following way. A uniform velocity profile U was introduced at the inlet boundary (the nozzle inlet). A free outflow condition at the outlet boundary and a zero velocity at the walls were also used. As far as temperature is concerned, both boundaries (walls and inlet) are

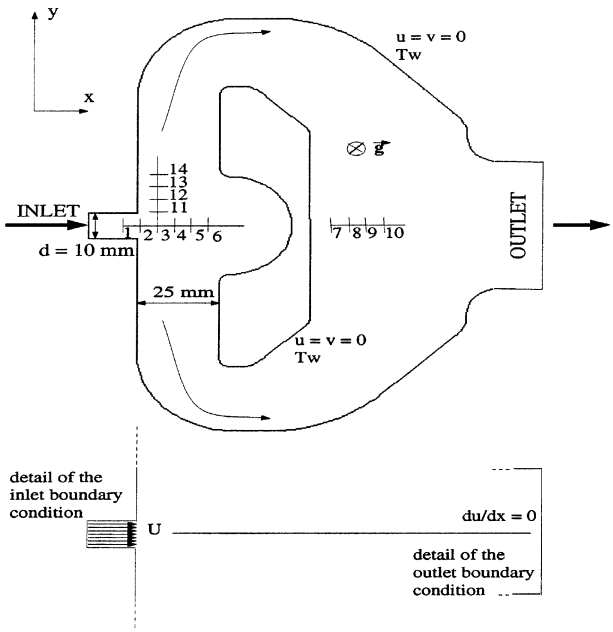

Figure 1. Physical domain, coordinate system and history points locations.

fixed at $T_{\text{wall}} = T_{\text{inlet}} = 293$ K in the dynamical study, and $T_{\text{wall}} = 303$ K in the thermal study. The Reynolds number is defined using U, the uniform velocity profile; d the nozzle width and ν the kinematic viscosity calculated for air in standard conditions. The simulations presented here are carried out for a distance $x = 25$ mm between the nozzle exit and the front of the bluff body.

The computations were performed as follows. For each Reynolds number, typically from 10 to 170, the steady solution is calculated and then taken as initial condition when the unsteady solutions are performed. A saturated periodic state is then obtained — which can be assimilated to an asymptotical regime — characterized with its peak-to-peak amplitude and frequency (see *figure 2*). Many previous methods are used with quite similar goals. Zielinska and Wesfreid [7] choose to compute the quasi-steady state solution until the time periodic state solution was reached. Therefore, by lowering step by step the Reynolds number and taking the saturated dynamics as an input, they obtained new stable time periodic fields. Bouchet [8] used as initial condition a steady symmetric flow called "basic flow" by forcing the symmetry artificially. Our method, described above, is chosen in order to analyze separately each computation.

We present here some results achieved according to different initial conditions. We take as initial condition an unsteady solution computed for $Re = 57$ in the saturated regime and then we increase slightly the Reynolds number ($Re = 60$). As expected, the saturated dynamics is reached faster than taking the steady solution as initial condition. This result does not present differences as far as saturated amplitude and frequency are concerned. In the same way, we choose the saturated state computed for $Re = 65$, as initial condition, and lower the Reynolds number ($Re = 60$). We obtain roughly the same results. The saturated amplitude is upward (approximately 2 %) in this last case, for the both components. The frequency is identical and independent of the chosen initial condition.

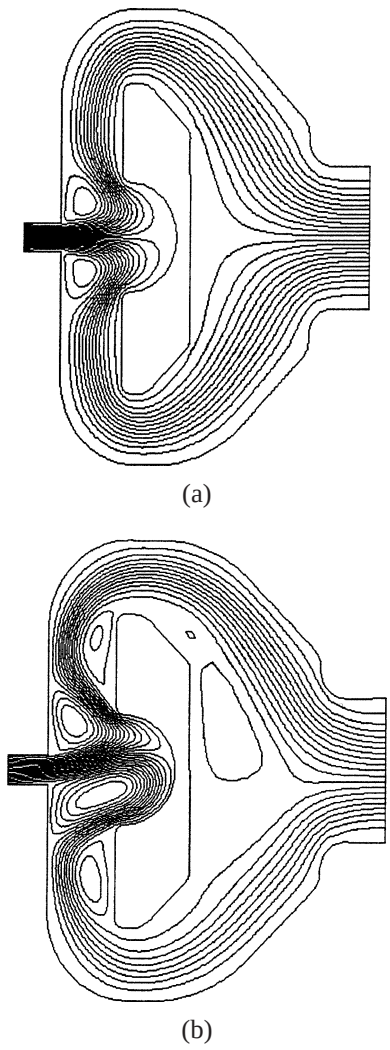

Figure 2. Flow pattern for both under and over critical Reynolds number.

Further computations were performed to optimize the appropriate grid. We studied the variation of the stream

TABLE I
Coordinates of the 14 history points.

Point	x/d	y/d
1	1	0
2	1.5	0
3	2	0
4	2.5	0
5	3	0
6	3.5	0
7	7	0
8	7.5	0
9	8	0
10	8.5	0
11	3	0.5
12	3	1
13	3	1.5
14	3	2

function and both velocity components with regard to *Nx* and *Ny*, the number of nodes in the longitudinal and transverse directions. For a chosen grid (Nx, Ny) and for a fixed Reynolds number ($Re = 70$), u, v and sf were calculated. Then, we increased *Nx* and the same quantities were calculated again (u_1, v_1 and sf_1). Each relative error (i.e. $(u_1 - u)/u$) has been analyzed and *Nx* is increased as long as this criterion is higher than 5 %. We proceeded in the same way for the *Ny* influence. The computational domain, which characteristics are $Nx = 106$ and $Ny = 162$, is chosen with respect to these constraints.

To identify the evolution and the growth characteristics of the velocity fields dependent on the Reynolds number (and the spatial locations x/d and y/d), we store the time evolution of the velocity components at the so-called history points. Saturated amplitudes are investigated at the 10 points on the symmetry axis ($y = 0$) and at 4 other points with a fixed crosswise location. These points are shown in *figure 1*. The coordinates expressed in relation with the nozzle width d (x/d for the 10 first points, y/d for the last 4) are given in *table I*. Points 1–6 and 11–14 are located upstream of the bluff body.

3. DETERMINATION OF THE THRESHOLD, CRITICAL BEHAVIOR

The system presented here is related to a horse shoe shape chamber and imply the instability of a confined jet. This system is found to undergo a transition from an oscillatory state at a critical Reynolds number. Through the temporal evolutions of the u and v components, we extract essential parameters to determine the onset of the self-excited phenomenon.

At $Re = 10$, the flow is symmetric (*figure 2*). The perturbations on the shear layer, which take place at the nozzle inlet exit, symmetrically, are not amplified and due to viscous damping, the flow is time independent. By increasing step by step the Reynolds number, we obtain quite similar behaviors, as far as $Re < 50$.

Close to $Re = 51$, temporal evolutions of both velocity components revealed a more complex behavior shown in the following figures. The flow symmetry is then broken (*figure 2*). According to linear stability theory, the transverse velocity is exponentially amplified with time during the first 800 s (*figure 3(a)*). This step is called the linear domain, where the linear terms of the momentum equation are prevailing. Then, the nonlinear terms, also amplified, inflect the exponential growth ($800\ \text{s} < t < 1\,120\ \text{s}$) leading to a saturated state ($t > 1\,120$ s). This last state can be represented through its saturated peak-to-peak amplitude $A_{\text{sat}} = \max(A) - \min(A)$ and its fundamental frequency f (see *figure 3(a)* and *(b)*). Through *figure 3(b)*, we note that this sequence is Reynolds dependent. The destabilization occurs earlier when the Reynolds number increased. In this last regime, we store the amplitude of the velocity time evolutions as a function of the space location and the Reynolds number. We show in *figure 4* the evolution of $(A_{\text{sat}})^2$, the saturated square amplitude, versus the Reynolds number.

It can be concluded that $(A_{\text{sat}})^2$ is in good proportionality with *Re*, near the threshold. The scaling law $A \sim (Re - Re_{\text{c}})^{1/2}$ is characteristic of a bifurcation which is demonstrated to be the supercritical Hopf type (Raghu and Monkevitz [9], Williamson [10], Goujond-Durand et al. [11]). This evolution, related to $(A_{\text{sat}})^2$, predicts the critical Reynolds number to be $Re_{\text{c}} = 51$. Above the value of 62 and up to 120, the evolution is quite different. Through a change in the slope, $(A_{\text{sat}})^2$ follows a new linear law (see *figure 5*), because of the strong gap with regard to the threshold. Above $Re = 120$, the evolution of the square saturated amplitude is not coherent with the past remarks. Further work is undertaken to support this allegation.

The determination of the linear growth rate is also an alternative to estimate the onset of the oscillatory phenomenon. As described above, during the first steps of the time evolution, both components vary with time, following an exponential law $v \sim \mathrm{e}^{\sigma t}$ where σ is the

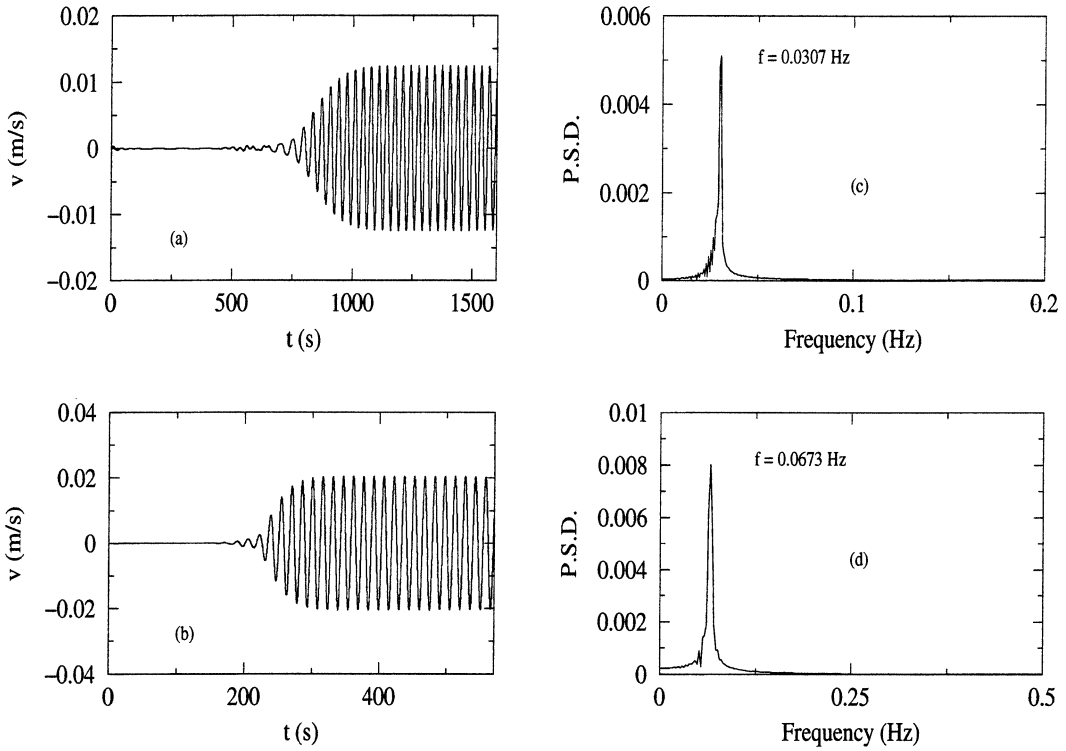

Figure 3. Temporal evolution of the spanwise component and associated spectrum, point 1, (a, c) $Re = 53$, (b, d) $Re = 60$.

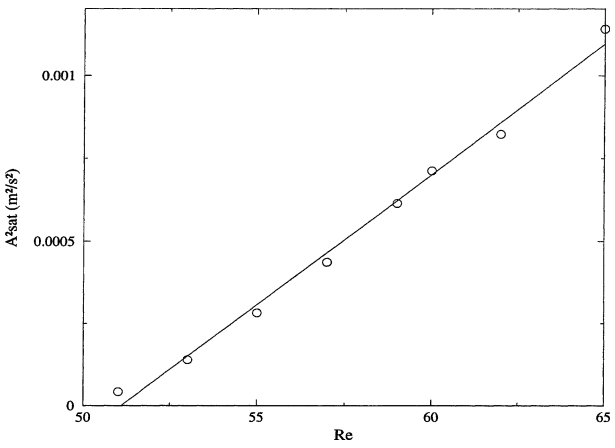

Figure 4. Square saturated amplitude versus Reynolds number, point 5.

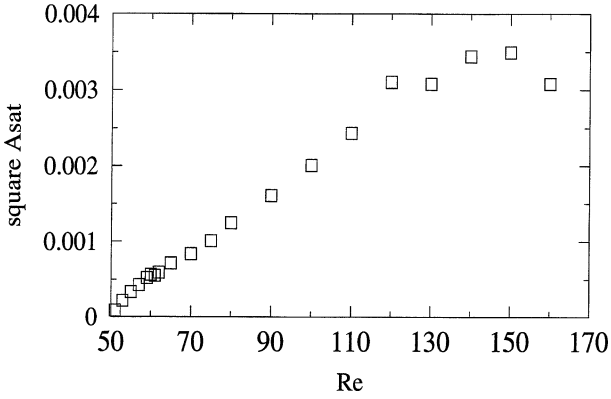

Figure 5. Square saturated amplitude versus Reynolds for the whole range, point 5.

linear growth rate. For each simulation, we compute, via a Hilbert transform, the envelope of the signal related to the transverse component, scaled with the ratio d^2/ν, expressed as a function of the Reynolds number. This linear law, extrapolated to the zeroth amplitude, gives the critical Reynolds number $Re_c = 49.9$. This value is in good agreement with the result obtained with the scaling law $A \sim (Re - Re_c)^{1/2}$. This difference can be explained by the difficulty to estimate the end of the linear regime, which defines the exponential law and, therefore, the linear growth rate σ. We also note that the results are similar whatever the spatial location is.

4. GLOBAL MODES

Many authors have shown that above a critical Reynolds number, wakes behind bluff bodies have a sufficiently large and absolutely unstable region to develop a global mode. This global mode is characterized by a self-sustained mechanism and a frequency independent with the spatial location. With the works reported in the last section, we are able to describe how the flow confined in the cavity loses its symmetry and reaches a new self-excited oscillatory state. We will first link this phenomenon frequency to the Reynolds number. Then, we will determine the shapes of the global modes.

In support of our interpretation, we study here, via a fast Fourier transform, the frequency of this self-excited mechanism, in a first step, as a function of the location (x/d) and then as a function of the Reynolds number. Our computations confirm that the frequency of the self-excited oscillation is constant whatever the location and the velocity component are. This result gives credence to the fact that the entire flow has a global behaviour. Frequency dependence with the Reynolds number is here studied. First, we present the results related to the transverse component on the symmetry axis. We note via *figure 3(a)* and *(b)* corresponding to $Re = 53$ and 60, respectively, that only one frequency appears on the spectrogram. This is a common result as far as the transverse component is concerned. We proceed in the same way for each Reynolds number. Results are projected on *figure 6*.

We note there are two zones where the frequency adopts a different evolution. First, close to the onset ($51 \leq Re \leq 61$), the frequency highly increases with the Reynolds number. Then, above $Re = 61$, as far as the frequency is concerned, the flow reaches a new state where its frequency variation is perfectly linear. In this part, the slope is equal to $\alpha_{\mathrm{NUM}} = 0.0018$ Hz$\cdot Re^{-1}$. This value is very close to the experimental one, $\alpha_{\mathrm{EXP}} = 0.002$ Hz$\cdot Re^{-1}$, obtained for an air jet flow in the same configuration over wider range of Reynolds numbers (600–30 000).

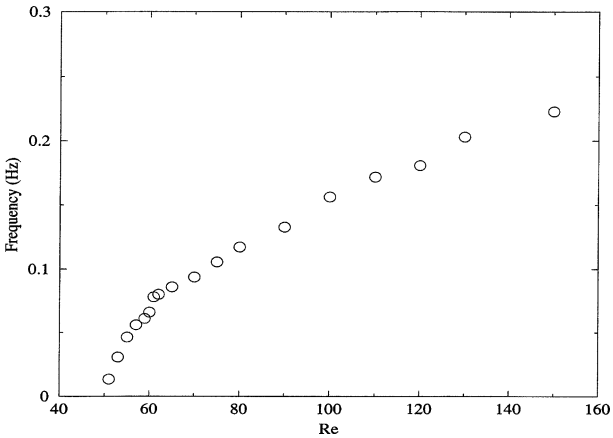

Figure 6. Evolution of the fundamental frequency versus Reynolds number, point 5.

As shown in *figure 7*, we can pay attention to the fact that the spectrogram linked to the longitudinal component (*figure 7(a)*) includes the first harmonic $2f$ and a particular mode related to the zeroth harmonic (the zeroth harmonic is not shown here). The harmonic $2f$ is the consequence of the stream function symmetry properties on the symmetry axis (Dusek et al. [10]).

The fundamental frequency is in good proportionality with the Reynolds number. As expected in terms of flow measurement, over $Re = 61$, the relation is linear and allows us to express the frequency as follows (Bouchet [8], Pacheu et al. [11], Maurel et al. [12]): $f = f_0 + \alpha Re$, where f_0 is the value for $Re = 0$ and has, of course, no physical meaning. It shows that the Strouhal number, dependent on the Reynolds number, is not constant but tends to an asymptotical value. This result is typical of Hopf bifurcations. We can define a particular Strouhal number, St_∞, which can represent the limit of the system at high inlet velocities:

$$St = \frac{f d}{U}, \qquad f = f_0 + \alpha Re$$

We can express the Strouhal number as follows:

$$St = \frac{f d}{U} = \frac{f_0 d^2}{\nu}\frac{1}{Re} + \frac{\alpha d^2}{\nu} = \frac{\beta}{Re} + St_\infty$$

The asymptotical value is, in the present case, $St_\infty = 0.00997$. This result, shown in *figure 9*, seems to be coherent with the experimental result obtained in the same configuration in a low speed water loop, which value $St_{\infty-\mathrm{exp}} = 0.0126$, over a wider Reynolds number range which can explain the difference between the two values. We know that there is a weak change for the frequency evolution as far as $Re \geq 70$. In our experimental work we actually are able to deal over a range of $100 \leq Re \leq 10\,000$.

For each Reynolds number allowing the self-sustained mechanism, we store at the history points the saturated amplitude of both velocity components u and v, respectively. Following up many papers (Zielinska et al. [13], Chapin et al. [14]), we choose to scale A_{sat}, the saturated amplitude, with A_{max}, its maximum value. We show, as

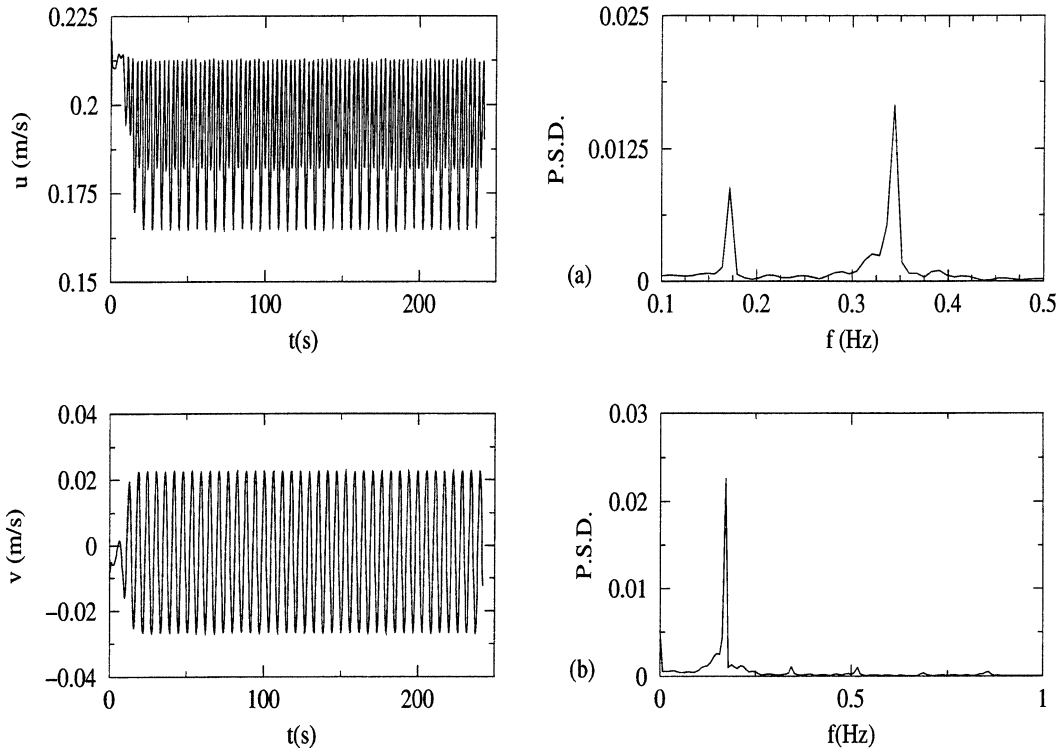

Figure 7. Time evolution and spectral density of the longitudinal (a) and transverse (b) components, $Re = 110$, point 1.

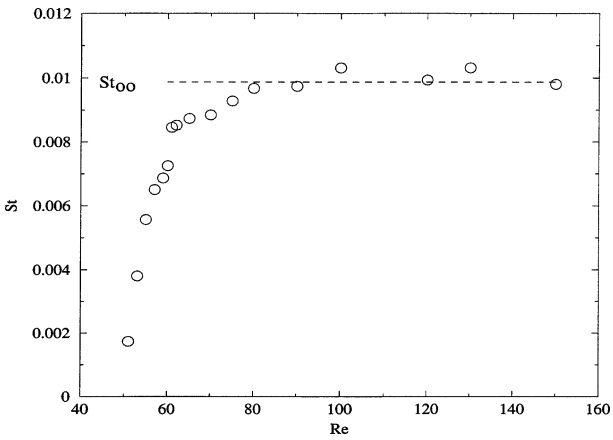

Figure 8. Evolution of the Strouhal number, point 5.

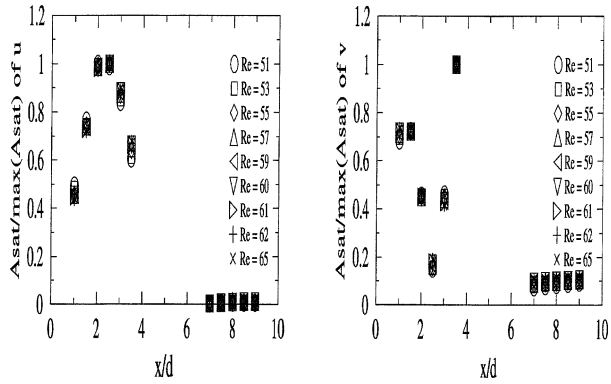

Figure 9. Rescaled amplitudes of the streamwise and spanwise components.

expected, that those evolutions follow an identical curve (see *figure 9* related to the longitudinal and transverse components u and v). These results traduce the fact that the flow behaves as a whole and follows the oscillatory movement in the entire domain. We can note how the energy moves to u component from v component. An increasing amplitude of the longitudinal velocity is here directly linked to a transverse velocity amplitude decrease. Obviously, $A_{\max}$ is a function of the Reynolds number, which is not really the case for $X_{\max}$, the abcissa where the amplitude reaches its maximum. We can say that $X_{\max}$ becomes Reynolds independent as soon as $\varepsilon \geq 0.04$, with $\varepsilon = (Re - Re_c)/Re_c$. We obtain an asymptotical value $X_{\max} = 3.5d$ with measurements of the transverse component. This result is in good agreement

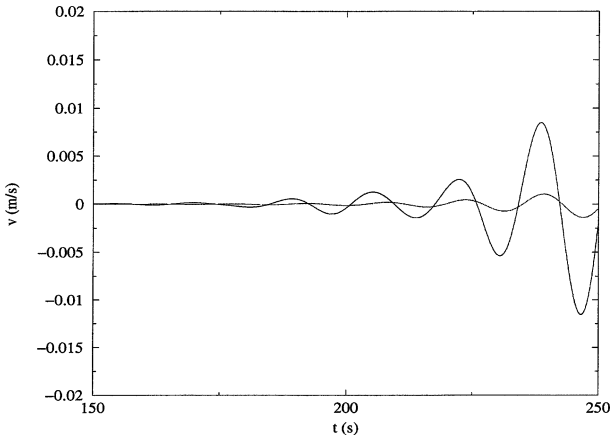

Figure 10. Comparison of the transverse component time evolution at an upstream (larger amplitude) and downstream location.

with the conclusions obtained experimentally in a different configuration by Goujon-Durand et al. [15]. The asymptotic regime is reached later (at about $\varepsilon = 0.5$), nevertheless, $X_{\max}$ is equal to $3.5d$.

Whereas the flow behaves as a whole, we have to note that the initial perturbation is first amplified upstream of the bluff body. Then, the self-excited mechanism affects the entire flow. Due to the central cavity, the phenomenon is more amplified, as shown in *figure 10*. Nevertheless, anything proves that the phenomenon first appears upstream. Further works are in progress to check it or not.

5. HEATING INFLUENCE

The numerical study described in the beginning of this paper has shown how a confined jet can exhibit self-sustained mechanism. We relate the frequency of this phenomenon with the inlet velocity and emphasize the global behavior of this confined flow.

It was clearly observed in early works that small changes in the geometry could reduce or alter the occurrence or the development of self-excited structures. Recent years have seen research related to the active control of many fluid mechanical systems. Experimentally and analytically, the use of a feedback control was investigated (Monkewitz [16]). It was concluded that self-sustained systems could be stabilized over a small range of Reynolds number. Therefore, many approaches were used in the domain of active control: base bleed and forced transverse cylinder oscillations by different authors (Rossopoulos [6]).

In terms of flow measurement, it is interesting to be able to detect low flow rates. Our system can be then limited by the onset of the oscillatory phenomenon. This threshold is directly linked with the viscous dissipation. Therefore, we present additional works related to the influence of the heating boundary on the self-excited phenomenon onset. The evolution of the global modes is also discussed here.

The numerical method used is the same as described above. The inlet flow temperature is kept constant $T_{\text{inlet}} = 293$ K. Each physical boundary (chamber walls, bluff body) is heated with a constant temperature varying between 303–333 K.

We choose the dynamic viscosity μ to be a linear function of the temperature T expressed by $\mu(T) = A_1 + A_2 T$. According to the physical properties of gases at atmospheric pressure, we determine A_1 and A_2 between 303 and 333 K (with $A_1 = 1.431{\cdot}10^{-5}$ kg·m^{-1}·s^{-1} and $A_2 = 1.84{\cdot}10^{-8}$ kg·m^{-1}·s^{-1}·K^{-1}. Other properties are chosen to be independent with the temperature.

As mentioned above, we compute the mass, momentum and energy equations for a range of Reynolds number between 50 and 140. We store at the history points, velocity components (u, v). Through their time evolution, we look for the conditions under which the flow can exhibit a self-excited pattern, characterized with its fundamental frequency, its saturated amplitude and, therefore, its global modes.

This part we will focus on the results obtained for $T_{\text{wall}} = 303$ K. Over $Re = 54$, time evolutions revealed an oscillating behavior, as proved in the dynamic study for Reynolds numbers higher than 51. We characterize this phenomenon through its saturated amplitude (see section 3). In *figure 11*, the evolution of $(A_{\text{sat}})^2$ versus the Reynolds number is plotted. Identically to the dynamic study, $(A_{\text{sat}})^2$ depends linearly on the Reynolds number. A critical value of $Re_{\text{c}} = 54$ is here obtained. A raise equals to 10 K for the walls temperature leads to an onset delay of about 6 %. It can be explained with the increase of the viscous damping with the temperature.

We extract the fundamental frequency of the oscillatory phenomenon. Close to the onset ($Re = 55$–65), this value highly increases with the Reynolds number. As in the dynamic study (see *figure 6*), we can see an inflexion of the slope over $Re = 65$ and then the frequency follows a linear law which can be expressed as follows: $f_{303} = f_{0-303} + \alpha_{303} Re$. Analyzing the difference between α and α_{303} gives an idea about the real influence of the walls heating. The slope obtained for $T_{\text{wall}} = 303$ K is 5 % higher than in the other case.

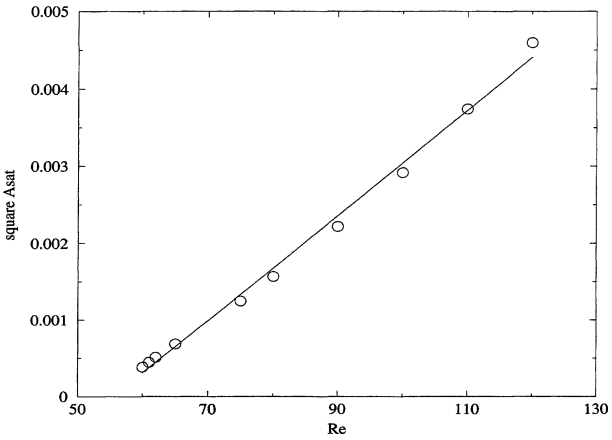

Figure 11. Square saturated amplitude versus Reynolds number, $T_{\text{wall}} = 303$ K, point 4.

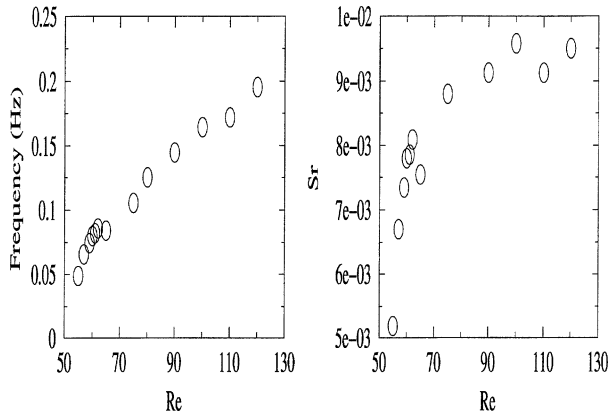

Figure 12. Evolution of the fundamental frequency and associated Strouhal number versus Reynolds number, $T_{\text{wall}} = 303$ K.

These results insist here on the fundamental role played by the viscosity by comparison with the nonheated cavity.

For each Reynolds number computed, we extract A_{sat}, the value of the saturated amplitude. This value decreases when $\Delta T = T_{\text{wall}} - T_{\text{inlet}}$ increases as shown in *figure 12*. When ΔT is higher than 10 K, the decreasing law is roughly linear which can predict the saturated amplitude behavior for higher temperature walls. Among these history points, the locations $x/d = 1$ (point 1) and $x/d = 3.5$ (point 6) are more subject to the heating influence because of their positions (see *figure 1*). We confirm experimentally the influence of the viscosity on the oscillatory phenomenon amplitude. When the water is the working fluid, the viscosity decreases with the increase of the temperature. Each increase of the amplitude is the result of a higher bluff body temperature. When T_{wall} is over 323 K, the velocity time evolutions are not monotonous. The saturated amplitude is reached after either a short decrease or an overtaking in its maximum value (see *figure 14*). As previously done, we present now $A_{\text{sat}}/\max(A_{\max})$ versus x/d at fixed Reynolds number and for different walls temperature $T_{\text{wall}} = 293$, 303, 313 K. These results are projected on *figure 15*. As shown in the dynamic study, each component follows an identical curve, independent with the Reynolds number and the walls temperature. These simulations have been done under the assumption of heated (303 and 313 K) and nonheated (293 K) wall boundaries which confirms its unsensitiveness to external thermal forcing.

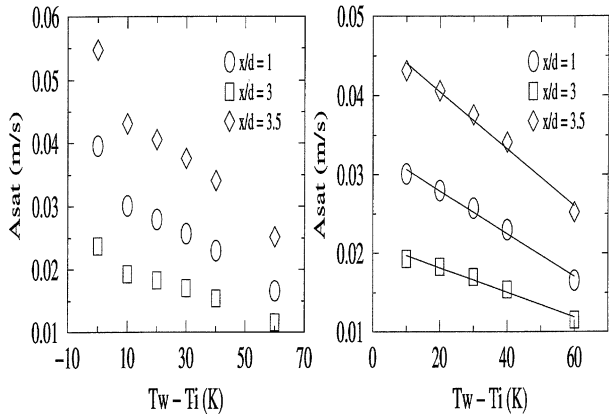

Figure 13. Decrease of A_{sat} for the transverse component, $Re = 60$.

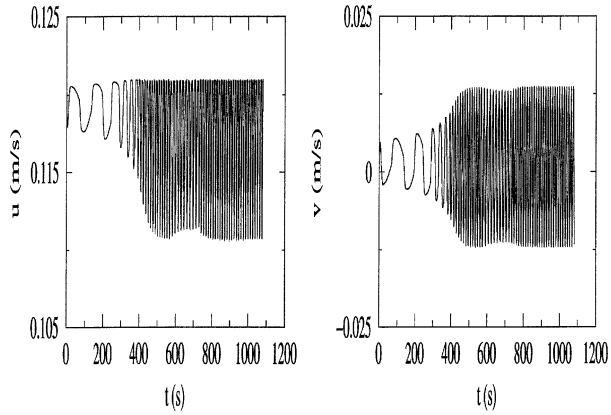

Figure 14. Time evolutions for the longitudinal and transverse velocities, $Re = 60$, $T_{\text{wall}} = 323$ K.

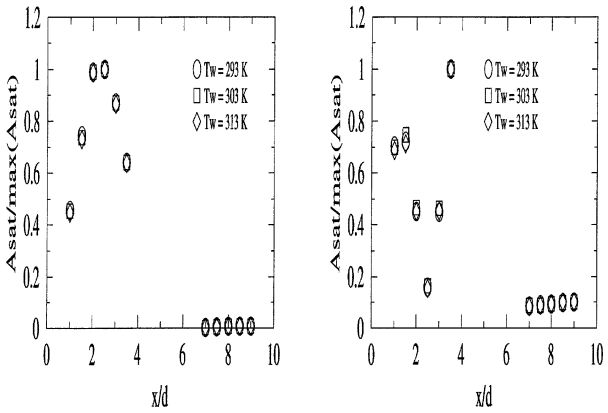

Figure 15. Rescaled amplitudes of the streamwise and spanwise components, $Re = 55$.

6. CONCLUSION

In this work, we have presented numerical simulations for a 2D jet confined in a horse shoe shape chamber containing a target crosswise to the main direction of the flow. Over $Re_c = 51$ in the dynamical study, the jet undergoes a Hopf bifurcation and reaches a new limit cycle state which is clearly described on frequency and saturated amplitude. We confirm further numerical and experimental results by building a scaling law for A_{sat} and f, with $A_{sat} \sim Re^{1/2}$ and $f \sim Re$. The last relation is of prime importance in terms of flow measurement, delivering a simple linear relation between the frequency and the inlet velocity, or the flow rate.

For each Reynolds number allowing self-sustained oscillations, we choose to scale the saturated amplitude with A_{max} its maximum value. Those evolutions follow an identical curve traducing the fact that the flow behaves as a whole in the entire domain. We define the saturated amplitude, the oscillations frequency and the so-called global mode.

It is necessary to detect flow rates as low as possible. Then we have presented an additional study related to the wall boundaries heating influence. A difference of 10 K between the walls temperature and the fluid temperature delays significantly the oscillations threshold by 6% ($Re_c = 54$ when $T_{wall} = 303$ K; $Re_c = 51$ when $T_{wall} = 293$ K), which is a consequence of the viscosity raise. Correspondingly, the saturated amplitude decreases with the walls temperature. Nevertheless, we pretend that the global mode patterns are not affected by this external heating, which shows the robustness of the global oscillation phenomenon.

Acknowledgements

We acknowledge technical and financial support provided by Gaz du Sud Ouest. Authors would like to thank Pr. F. Charru (IMFT) for his enlightening help.

REFERENCES

[1] Huerre P., Spatio-temporal instabilities in closed and open flows, in: Instabilities and Nonequilibrium Structures, D. Reidel Publishing Company, 1987, pp.141–177.

[2] Provansal M., Mathis C., Boyer L., Bénard–von Karman instability: transient and forced regimes, J. Fluid Mech. 182 (1987) 1–22.

[3] Monkewitz P.A., Berger E., Schumm M., The nonlinear stability of spatially inhomogeneous shear flows, including the effect of feedback, Eur. J. Mech. B Fluids 10 (1991) 295–300.

[4] Rockwell D., Naudasher D., Self-sustained oscillations of impinging free shear layers, Ann. Rev. Fluid Mech. 11 (1979) 67–94.

[5] Yu M.H., Monkewitz P.A., Oscillations in the near field of a heated two-dimensional jet, J. Fluid Mech. 255 (1993) 267–296.

[6] Roussopoulos K., Feedback control of vortex shedding at low Reynolds number, J. Fluid Mech. 255 (1993) 323–347.

[7] Zielinska B.J.A., Wesfreid J.E., On the spatial structure of global modes in wake flows, Phys. Fluids 7 (1995) 1418–1424.

[8] Bouchet G., Étude expérimentale et numérique des auto-oscillations d'un jet confiné, Ph.D. Thesis, Université Paris VI, France, 1996.

[9] Raghu S., Monkevitz P.A., The bifurcation of a hot round jet to limit-cycle oscillations, Phys. Fluids A 3 (1991) 501–503.

[10] Williamson C.H.K., Vortex dynamics in the cylinder wake, Ann. Rev. Fluid Mech. 28 (1996) 477–539.

[11] Dusek J., Le Gal P., Fraunie P., A numerical and theoretical study of the first Hopf bifurcation in a cylinder wake, J. Fluid Mech. 224 (1994) 59–80.

[12] Pacheu T., Le Guer Y., Lalanne L., Creff R., Étude experimentale des auto-oscillations d'un jet plan confiné au sein d'une cavité contenant un obstacle, C. R. Acad. Sci. Paris (1999) (submitted).

[13] Maurel A., Ern P., Zielinska B.J.A., Wesfreid J.E., Experimental study of self-sustained oscillations in a confined jet, Phys. Rev. E 54 (1996) 3643–3651.

[14] Chapin V., Bennazouz S., Chassaing P., On the spatial structure of global modes in two-dimensional heated jets, in: 29th American Institute of Aeronautics and Astronautics Fluid Dynamics Conference, Albuquerque, June 15–18, 1998.

[15] Goujon-Durand S., Jenffer P., Wesfreid J.E., Downstream evolution of the Bénard–von Karman instability, Phys. Rev. E 50 (1994) 308–313.

[16] Monkewitz P.A., The absolute and convective nature of instability in two-dimensional wakes at low Reynolds numbers, Phys. Fluids 5 (1998) 999–1006.